Raman spectroscopy of $La_2@C_{80}$ and $Ti_2@C_{80}$ dimetallofullerenes

R. Jaffiol, A. Débarre,* C. Julien, D. Nutarelli, and P. Tchénio
Laboratoire Aimé Cotton, CNRS, Bâtiment 505, 91405 Orsay cédex, France

A. Taninaka, B. Cao, T. Okazaki, and H. Shinohara
Department of Chemistry, Nagoya University, Nagoya 464-8602, Japan

(Received 15 October 2002; revised manuscript received 27 February 2003; published 10 July 2003)

This paper is devoted to the Raman spectroscopy of two dimetallofullerenes $La_2@C_{80}$ and $Ti_2@C_{80}$. Previous studies of monometallofullerenes ($M@C_{82}$) and dimetallofullerenes ($M_2@C_{82}$) have demonstrated that Raman spectroscopy is a useful tool to probe the cage-metal bond strength. The latter is a fingerprint of the metal to fullerene charge transfer, which plays an important role in the stabilization of the metallofullerene. In the present study, the metallic ions are trapped inside a C_{80} hollow cage for each metallofullerene, but their group and weight differ. This provides the opportunity to probe in the same study the ability of Raman spectroscopy to determine the ionization state of ions trapped in a cage, which eventually differs only by isomerization. A detailed analysis of the low-frequency part of the Raman spectrum is proposed for both $La_2@C_{80}$ and $Ti_2@C_{80}$. Two low-frequency modes at 161 cm^{-1} for $La_2@C_{80}$ and at 196 cm^{-1} for $Ti_2@C_{80}$ are tentatively assigned to a fingerprint of the interaction between the trapped ions and cage. The corresponding values for the metal-cage valence force constant are in favor of an effective charge transfer of three electrons per lanthanum to the cage and of two electrons at most per titanium to the cage. These results are in good agreement with theoretical predictions and with electron energy loss spectroscopy or x-ray observations.

DOI: 10.1103/PhysRevB.68.014105 PACS number(s): 78.30.−j, 78.30.Na

I. INTRODUCTION

Much effort has been devoted to further production, extraction, purification, and separation of metallofullerenes (MF's) after the first production of a stable species, $La@C_{82}$ in solution.[1] Apart from the most widely studied metallofullerenes involving group II, group III, or lanthanide metals, MF's associating nitrogen to these metals have been recently extracted with a high yield.[2] The possibility of trapping ions or atoms in hollow fullerene cages has attracted a large interest theoretically and experimentally. Recent reviews nicely summarize the status of the art in this ten-years-old research field.[3,4] The clear confirmation of the endohedral location of the metallic species in the fullerene cage was first demonstrated in the case of $Y@C_{82}$ by an x-ray structural study.[5] The maximum entropy method (MEM) combined with the analysis of synchrotron powder diffraction data was then used to retrieve information on the metal-cage interactions. Particular attention was paid to charge transfer, which plays a major role in stabilizing the metallofullerenes.[6] This study pointed out that the cage structure of a metallofullerene might differ from the structure of the relevant most abundant hollow fullerenes. In particular, the metal-cage interactions can favor stabilization of minor isolated pentagonal rule (IPR) isomers or even non-IPR isomers satisfying cage structures, as predicted for $Ca@C_{72}$, for example.[7]

The relation between the oxidation state of the encaged atoms, the stability, and the nature of the dominant trapping cage isomer is of particular interest to understand the elaboration process and the reactivity properties of the relevant species.[7,8] Recent studies aim at demonstrating that the carbon cage symmetry is specific towards the ionization states of the encaged metals and, in particular, that the stable cage for a 2+ metallic ion is not the most stable cage for a 3+ one.[9] Nevertheless, due to the difficulty in isolating large enough quantities for most MF's, experimental results are often still lacking or incomplete to corroborate theoretical predictions.

Raman spectroscopy is an alternative method that can help us derive informations on metallofullerene symmetry and metal-cage bond strength. Recently, new insight into MF vibrations was deduced from detailed analyses of Raman spectroscopy studies in conjunction with IR spectroscopy and with neutron scattering. It concerned the $M@C_{82}$ series with $M=$ La, Y, Ce, Gd (Ref. 10) and different isomers of $Sc_2@C_{84}$ and $Tm@C_{82}$ (Ref. 11). In all cases, the authors paid specific attention to the fingerprints of the metal-cage interaction. They also derived an experimental value of the metal-cage bond strength from a simple picture that describes the relevant vibration as a harmonic oscillator. The bond strength value depends on the ionization state of the encaged metallic ions. As a result, spectroscopy can be used as an alternative method to identify the ionic charge of the metallofullerenes. A force constant value close to 1.2 N/m is characteristic of divalent ions (Sc, Tm), whereas a force constant value of the order of 1.8 N/m is obtained for trivalent ions (La, Gd, Ce). Furthermore, the studies of Ref. 11 involve three different isomers for $Sc_2@C_{84}$. The results demonstrate that there are some differences in the Raman spectra of the various isomers for a given dimetallofullerene. The differences are more important than those observed for the isomers of the hollow cage, but line shifts are still of the order of 10 cm^{-1}.

The present study is devoted to the Raman spectroscopy of both $La_2@C_{80}$ and $Ti_2@C_{80}$ at room temperature. $La_2@C_{80}$ has been extracted successfully nearly ten years ago. Nevertheless, no Raman study has been performed on such dimetallofullerenes. In contrast, the extraction of

$Ti_2@C_{80}$ was reported only very recently.[12] It is the first demonstration of metallofullerenes entrapping atoms of the group IV. Many structural data on $La_2@C_{80}$ are available, but there are only few data on $Ti_2@C_{80}$. In both cases, the metallic atoms are trapped inside a C_{80} fullerene. In the case of $La_2@C_{80}$, the cage isomer has the symmetry I_h. Here $Ti_2@C_{80}$ corresponds to a mixture of two isomers of the cage of symmetry I_h and D_{5h}, respectively.[12,13] One aim of this paper is to use the correlations between the Raman spectra recorded for $La_2@C_{80}$ and $Ti_2@C_{80}$ to retrieve information on the Raman signatures relevant to the carbon cage vibrations alone and on those corresponding to metal-cage interactions since both the weight of the trapped metals and their group differ. In order to disentangle the complex spectra, we have used as a starting point an empirical model that correlates the C_{80} cage modes to the C_{60} ones as in previous studies.[11] It has been demonstrated that the frequencies of some modes of fullerenes larger than C_{60}, in the low-frequency domain, can be deduced in a first approximation from those of C_{60} modes by a scaling law involving the mass of the cage. A detailed comparison between the spectra of $La_2@C_{80}$ and that of $Ti_2@C_{80}$ is derived in the low-frequency domain. The relation between the force constants of the metal-cage vibrations and the atom ionization state is discussed for both La and Ti. These values are compared to previous data.[10,14,15]

II. SAMPLE PREPARATION AND MEASUREMENT

The Raman spectra were recorded on a homebuilt confocal spectrometer, described elsewhere.[16] The collection is performed in a backscattering configuration. In the present study, no surface-enhanced Raman scattering (SERS) is used. The excitation at 514 nm is provided by an argon laser. The laser is focused through a 100×, 1.3 numerical aperture (NA) immersion objective to a diffraction-limited spot with a diameter of the order of 400 nm. The plasma lines of the laser are removed by using either an excitation filter or the combination of an excitation filter and of a prism premonochromator. Notch filters are used to select the Raman signal that is detected on an N_2-cooled camera through a single-pass monochromator. Spectral resolution is 4 cm^{-1}. The metallofullerenes are produced in the group of H. Shinohara. This group has previously described in detail the isolation process of $La_2@C_{80}$ and $Ti_2@C_{80}$ (Refs. 12 and 22). These species are further stocked in CS_2. Two types of samples were prepared for studying $La_2@C_{80}$. In the first kind of sample, $La_2@C_{80}$ dispersed in CS_2 is gently sonicated for 1 hr, then, the solution is filtered through a 0.5-μm pore membrane and finally drop coated on a clean glass substrate. The sample is kept at room temperature since $La_2@C_{80}$ is stable in air. The final spectrum is generally obtained by adding several spectra recorded with an acquisition time of 60 s in order to get a high enough signal-to-noise ratio. This kind of sample will be labeled S_1. The second kind of sample corresponds to $La_2@C_{80}$ in solution in toluene. A drop of $La_2@C_{80}$ dispersed in toluene is trapped within two clean microscope cover plates. The thickness of the sample of MF's in solution is of the order of 10 μm. As a result, overall acquisition times of the order of 20–30 min are required to obtain a sufficient signal-to-noise ratio on such samples. This kind of sample is labeled S_2. Data on $Ti_2@C_{80}$ have only been studied in solution in dichloroethane with a sample preparation similar to that described above for $La_2@C_{80}$ S_2 samples. For all samples, the intensity of the laser beam was maintained below the limit of 1 mW/μm^2. A larger intensity causes a degradation of the signal-to-noise ratio, especially in the case of the S_1 sample, both because of an excessive heating of the sample and because of the rather low photostability of MF's.

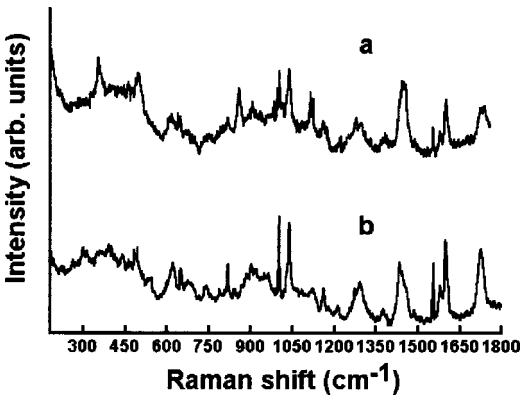

FIG. 1. Raman spectra of $La_2@C_{80}$ in toluene (a) and of $Ti_2@C_{80}$ in dichloroethane (b).

III. RESULTS

The Raman spectra of $La_2@C_{80}$ and $Ti_2@C_{80}$ S_2-type samples are shown in Fig. 1 on a spectral domain ranging from 180 to 1900 cm^{-1}. Three successive spectra are acquired in 800 cm^{-1} largely overlapping domains in order to obtain the Raman signal on this broad spectral range. The acquisition time is 60 min for each spectrum. As expected from the higher number of carbons in the C_{80} cage, both spectra exhibit more complicated features than C_{60} or C_{70} spectra, especially in the high-frequency part of the spectra where numerous lines including combination lines merge into broad structures. In order to get a high enough signal-to-noise ratio in these diluted samples, it was necessary to derive a compromise between a severe filtering of the Raleigh signal and an efficient collection of the signal. As a result, lines between 150 and 200 cm^{-1} appear as weak shoulders on an increasing background and they can only be recovered by deconvolution from the Raleigh signal.

As expected, the overall features of the high-frequency part above 900 cm^{-1} are very similar for both spectra. The relevant modes correspond to hard-tangential vibrations of the C_{80} cage. They depend little on the encapsulated species. The $La_2@C_{80}$ spectrum was fitted with Lorentzian-shaped lines in the range 900–1750 cm^{-1}. Then the same set of lines was used to fit the $Ti_2@C_{80}$ spectrum. Figure 2 demonstrates that the $Ti_2@C_{80}$ spectrum can indeed be correctly fitted with almost the same set of frequencies in this frequency range. Nearly any line in one spectrum has its counterpart in the other, but the relative intensities of the modes are some-

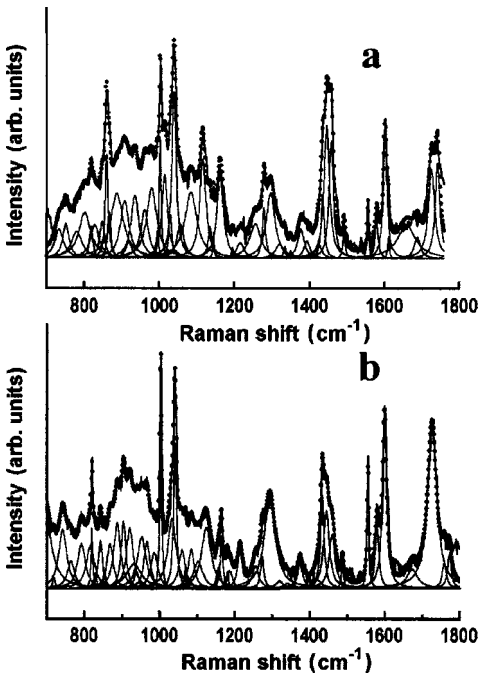

FIG. 2. Fit of the Raman spectra of the dimetallofullerenes in solution in the intermediate- and high-frequency domains. (a) and (b) correspond to $La_2@C_{80}$ and $Ti_2@C_{80}$, respectively. The solid circles display the total fit. The solid lines display the individual Lorentzian-shaped curves used in the fits.

times different and some minor shifts occur. This clearly appears for the structure around 1450 cm^{-1}, for which the intensities of the lines are stronger for $La_2@C_{80}$ than for $Ti_2@C_{80}$. Some differences are observed in the domain around 1750 cm^{-1}. But this last effect can be largely attributed to a contribution of the combination modes. These contributions are different for the two metallofullerenes since they imply low-frequency modes that are metal specific. The close similarity of both spectra in the high-frequency range, where the cage modes dominate, indicates that the influence of the isomerism of the cage is weak in agreement with previous results for the isomers $Sc_2@C_{84}$ and $Tm@C_{82}$ (Ref. 11). This observation is consistent with the fact that the involved isomers of the C_{80} cage, D_{5h} and I_h, are very similar in shape and that the latter is present in $La_2@C_{80}$ and $Ti_2@C_{80}$. However, there are some differences. First, the intensity ratio of the thin lines at 1041 and 1004 cm^{-1} are reversed in $La_2@C_{80}$ and $Ti_2@C_{80}$. Three sharp lines appear in the spectrum of $Ti_2@C_{80}$ at 1181, 1158, and 1070 cm^{-1} that are not present in that of $La_2@C_{80}$. These three lines could be fingerprints of the D_{5h} isomer of $Ti_2@C_{80}$. One could have expected to observe more differences in the middle- and high-frequency domains between $Ti_2@C_{80}$ and $La_2@C_{80}$ spectra because the D_{5h} isomer has a lower symmetry than the I_h.

The dimetallofullerene spectra display more differences in the intermediate region ranging from 700 to 900 cm^{-1}. In the range 800–900 cm^{-1}, all lines still have a counterpart in either spectrum, but their intensities are often rather different. It is the case of the thin line at 860 cm^{-1}, which is much stronger in the $La_2@C_{80}$ spectrum than in the $Ti_2@C_{80}$ one and the reverse for the line at 920 cm^{-1} (see Fig. 2). In the range 700–800 cm^{-1} the spectra of both species differ, indicating that the perturbation of the cage modes by the trapped ions is no longer negligible. A different splitting of the modes is clearly observed.

IV. DISCUSSION

This discussion is devoted to an analysis of the low-frequency part of the Raman spectra, where some of the differences between $La_2@C_{80}$ and $Ti_2@C_{80}$ spectra are expected to be fingerprints[10,11] of the encaged metal atoms and of their interaction with the C_{80} cage. Moreover, one gets the opportunity of deriving values of the strength of the bond between the metallic ions and the cage from the frequency of such lines. This value is a signature of the ionization state of the encapsulated species.[15]

We first consider the case of $La_2@C_{80}$. $La_2@C_{80}$ was first detected by mass spectrometry in 1991.[17] $La_2@C_{80}$ is obtained as a by-product of the synthesis of $La@C_{82}$. It is extracted only in small amounts. Consequently, fewer experimental data are available than in the case of $La_2@C_{82}$ or in the case of $Sc_2@C_{84}$, for example. Moreover, $La_2@C_{80}$ is electron paramagnetic resonance (EPR) silent. Nevertheless, it has been successfully studied by electrochemistry.[18] The results demonstrate that the $La_2@C_{80}$ dimetallofullerene behavior differs from that of $La@C_{82}$ major and minor isomers. $La_2@C_{80}$ has also been theoretically studied[19] as well as the symmetry properties of the hollow C_{80} (Ref. 20). Finally, the properties of $La_2@C_{80}$ have also been studied when it is encapsulated in nanotubes to form so-called peapods.[21] C_{80} has seven isomers that satisfy the IPR rule. Among them, the most stable are the D_{5d} and D_2 ones. They are the major isomers for the hollow cage. When two La atoms are trapped inside the C_{80} cage, the ionization state of each La is 3+. This has been recently observed by x-ray diffraction.[22] The six highest occupied molecular orbits (HOMO's) are then fully occupied, and the close-shell electronic configuration ensures the stability of $La_2@C_{80}$. The most stable cage compatible with $(La^{3+})_2C_{80}{}^{6-}$ is the most symmetrical one, the I_h-C_{80}, which is different from the cages of the major isomers of the hollow C_{80} cage.[19] The negative charge on C_{80} plays a major role in the relative stability of the different isomers. The vibrational modes of I_h-C_{80} correspond to the symmetry types $3A_g+4F_{1g}+5F_{2g}+8G_g+11H_g+1A_u+6F_{1u}+7F_{2u}+8G_u+9H_u$. There are 14 Raman-active modes corresponding to $3A_g+11H_g$. In this structure, La atoms are aligned along the C_2 axis. The axis joins the centers of opposite six-membered rings of I_h-C_{80}. The symmetry of $La_2@C_{80}$ is thus predicted to be D_{2h}. This is supported by an analysis of the ^{13}C NMR spectrum of $La_2@C_{80}$ (Ref. 23) and by a synchrotron radiation structural study.[22] The predicted La-La and La-cage distances are 3.655 and 2.598 Å, respectively,[19] whereas the observed ones are 3.84 and 2.39 Å, respectively.[22] A weak covalent bond between the two La might be expected, but experiment is in favor of a weak ionic bond. The bond of each La atom with the cage is stronger and of ionic type.

This implies a lowering of the symmetry of the I_h-C_{80}

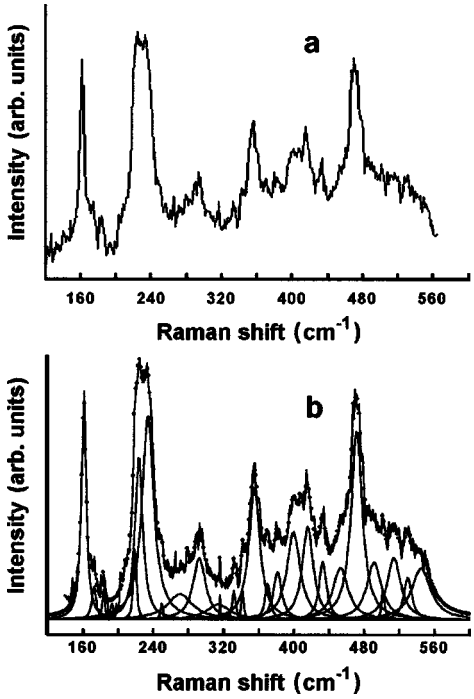

FIG. 3. Raman spectrum of $La_2@C_{80}$ solid (S_1 sample) in the low-frequency domain. (a) and (b) correspond to the raw data and relevant fit; respectively. The solid circles display the total fit. The solid lines display the relevant individual Lorentzian-shaped curves. The relevant frequencies are listed in Table I.

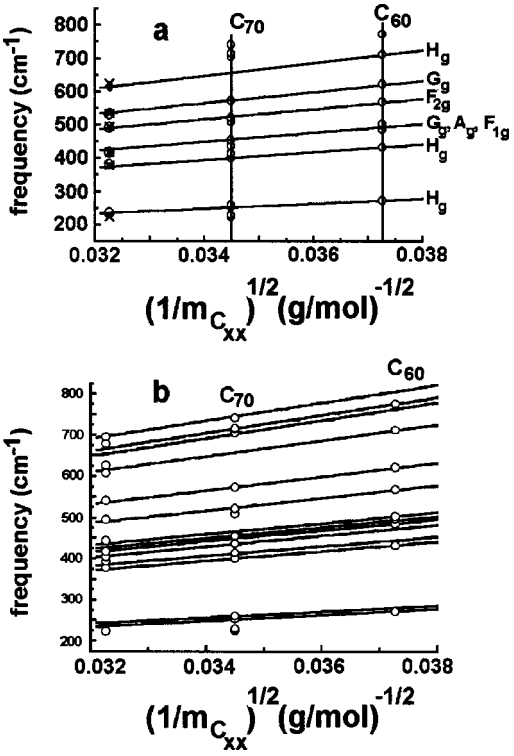

FIG. 4. Graphical determination of the C_{60}-related modes for the C_{80} fullerene. (a) Solid lines: linear regression fits of the cage mode frequencies vs the reciprocal square root of the cage mass m, based on the known mode frequencies of C_{60} and C_{70} (Refs. 24 and 26). Open circles on the vertical lines related to $m_{C60}^{-1/2}$ and to $m_{C70}^{-1/2}$, respectively, display these frequencies. Mode symmetries have been added in (a). On the vertical line corresponding to $m_{C80}^{-1/2}$ are displayed by large and small open circles and crosses, respectively, the experimental frequencies of the lines of the $Ti_2@C_{80}$ spectrum in solution, of the $La_2@C_{80}$ spectrum in solution, and of the solid $La_2@C_{80}$ spectrum, which nearly match the predicted values. Additional linear fits corresponding to C_{70}-related modes are displayed in (b). On the vertical line corresponding to $m_{C80}^{-1/2}$, open circles display the frequencies of the $Ti_2@C_{80}$ spectrum in solution that nearly match the predicted values.

cage, which leads to the following splitting of the cage modes:

$$A_g \rightarrow A_g,$$

$$F_{1g} \rightarrow B_{1g} + B_{2g} + B_{3g},$$

$$F_{2g} \rightarrow B_{1g} + B_{2g} + B_{3g},$$

$$Gg \rightarrow A_g + B_{1g} + B_{2g} + B_{3g},$$

$$Hg \rightarrow 2A_g + B_{1g} + B_{2g} + B_{3g}. \quad (1)$$

The A_g, B_{1g}, B_{2g}, and B_{3g} modes are all Raman active.

In order to disentangle the low-frequency part of the spectrum, we have first analyzed the typical spectrum acquired for an S_1-type sample. Such a spectrum is displayed in Fig. 3. It results from the superposition of four successive spectra, each acquired during 1 min. No major change was observed between the first and last acquisitions confirming the high enough stability of $La_2@C_{80}$ even at room temperature. In these recordings, it was easier to limit the background intensity by reducing the excitation power than for S_2 samples. Consequently, spectrum acquisition could be extended down to 120 cm^{-1} with a satisfactory signal-to-noise ratio.

As mentioned above, we have used the empirical mass scaling law in order to clarify the spectrum and then to tentatively identify modes, which depend on the interaction of the metallic ions and fullerenes. The basic assumption of this scaling law is that, in the low-frequency domain ($<700-750$ cm^{-1}), the frequency of a given mode varies smoothly from one cage to the other. More precisely, its frequency is inversely proportional to $M^{1/2}$, where M is the cage mass. This assumption has been verified on the frequency modes of C_{60}, C_{70}, C_{82}, and C_{84}. At first order, this approximation is also supported by the weak influence of the isomer on the low frequencies of a given species, as has been observed.[11] As a result, this scaling law can be used to predict the values of the C_{80} modes in the relevant frequency range up to 750 cm^{-1}. They can be derived from the frequency values of the low-frequency C_{60} modes.[24–27] Among these modes, four are Raman active in the considered range: namely, the three lowest H_g modes and the radial breathing mode $A_g(1)$.[24] Because of the lowering of the symmetry to D_{2h}, the modes related to the first-order silent modes of F_{1g}, F_{2g}, and G_g symmetries in C_{60} must also be considered. The relevant frequency values of C_{70} can also be used in the linear fits as shown in Fig. 4(a). These C_{70} frequencies were determined in previous studies.[25–29] The mass scaling law implies that

TABLE I. Frequencies and relative intensities for modes of $La_2@C_{80}$ between 150 and 500 cm^{-1}, sample S_1. Frequency values close to those of the C_{60}-related modes are labeled in bold characters. The intensity of the line at 161 cm^{-1} is taken equal to unity.

ω (cm^{-1})	Relative intensity
491	**0.27**
471	0.89
453	0.25
433	0.28
416	**0.44**
399	0.41
381	**0.23**
370	0.17
355	0.62
342	0.15
332	0.14
314	0.07
292	0.29
270	0.12
250	0.09
234	**0.97**
224	0.77
219	0.36
183	0.14
173	0.16
161	1.00

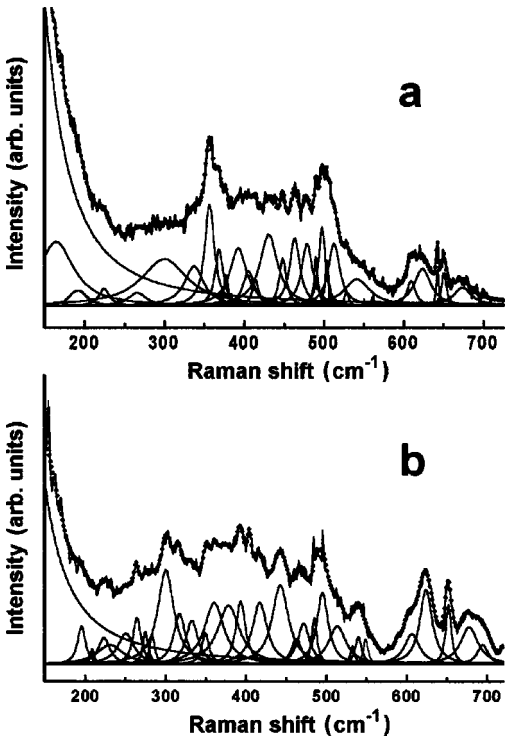

FIG. 5. Fits of the low-frequency domain of the Raman spectra of $La_2@C_{80}$ (a) and $Ti_2@C_{80}$ (b) in solution. Solid circles display the total fit curve. Solid lines display the individual Lorentzian-shaped curves which compose the fit. The relevant frequencies are listed in Table II.

the linear fits nearly go through zero, which would correspond to a fullerene of infinite mass. We can derive six values of C_{60}-related modes for the hollow C_{80} from the linear fits [Fig. 4(a)]. The frequencies are respectively 236, 374, 426, 490, 536, and 615 cm^{-1}. Table I lists the values of the lines observed in the S_1 sample. We observed a line at 416 cm^{-1}, which can be tentatively assigned to an A_g mode. In fact, the modes of A_g symmetry are not degenerate and keep the same symmetry in the D_{2h} group. This explains the fact that the A_g C_{60}-related mode can be observed. The spectrum displays a strong line at 235 cm^{-1}, which coincides with the predicted value of the $H_g(1)$ C_{60}-related mode. This mode has been also observed in the case of $Sc_2@C_{84}$ (Ref. 11). Two additional thin and strong lines are downshifted to 224 and 219 cm^{-1}. As they are close to the 235-cm^{-1} line, these modes can be tentatively assigned also to the splitting of the Hg(1) C_{60}-related mode. The Hg(1) mode splitting is expected because of the lowering of the symmetry to D_{2h}. The 235-, 224-, and 219-cm^{-1} lines can correspond to an incompletely resolved structure. Finally, we observe a mode at 161 cm^{-1} that has been also previously observed in the case of $La@C_{82}$ (Ref. 10). This mode was interpreted as a fingerprint of the interaction of La^{3+} with the C_{82} cage. In the present situation, if we assume that this mode is a fingerprint of the interaction of La^{3+} with the C_{80} cage, we can evaluate the force constant of the La-C_{80} bond by using a simple harmonic-oscillator model as in previous studies.[10,11] In fact, at room temperature, the two La atoms (ions) move along the dodecahedron trajectory of C_{80}. Under these circumstances, the La-La coupling is smaller than the La-cage interaction. Thus the frequency of the La-cage mode is given by

$$\omega \ (\mathrm{cm}^{-1}) = 4.12 \sqrt{\frac{k1}{m} + \frac{2k_1}{M}}, \tag{2}$$

where k_1 corresponds to the force constant of the La-C_{80} bond expressed in N/cm. M and m are the C_{80} molecular mass and the La atomic mass, respectively, expressed in kg. The value of the force constant in dyn/cm is $10^5 k_1$. For $\omega = 161\ cm^{-1}$, $k_1 = 1.63$ N/cm. This value is compatible with a 3+ ionization state of lanthanum, as expected.[10,14,15] Finally, in the range 355–545 cm^{-1} there are 12 lines apart from that at 416 cm^{-1}. In this frequency range, three C_{60}-related modes are expected at 374, 490, and 536 cm^{-1}. These modes are derived from H_g, F_g, and G_g modes, respectively, which are expected to split into five, three, and four modes, respectively. The observed number of modes is compatible with this description.

We then compare these results with those obtained for $La_2@C_{80}$ in solution. Apart from the contribution of the residual Raleigh scattering, the first characteristic of this low-frequency part of the spectrum compared to the previous one is the modification of the intensity distribution of the lines. Only a limited number of lines appears on a structured background. Two features dominate this spectrum. The first one at 355 cm^{-1} presents a shoulder more pronounced than in the S_1 spectrum. The second one, centered on 498 cm^{-1}, is much broader than its counterpart in the S_1 sample. In order to

TABLE II. Frequencies and widths (second number) for modes of $La_2@C_{80}$ and $Ti_2@C_{80}$ in solution, between 180 and 750 cm^{-1}, samples S_2. The weak lines are indicated by w in the same column. Second and fourth columns: possible contributions of combination modes. The frequencies labeled in bold characters correspond to the lines that appear only in one of the spectra.

$La_2@C_{80}$ in solution (cm^{-1})	Combination modes (cm^{-1})	$Ti_2@C_{80}$ in solution (cm^{-1})	Combination modes (cm^{-1})
		742 26	514+226, 494+250
733 28	512+224, 377+356		
699 34	478+224	695 17	494+196
681 7	478+224	678 27	
671 14	448+224		
651 7	430+224		
623 25		624 19	374+250
609 12		607 23 w	
541 40		546 7 w	316+226
		540 10 w	
528 6		533 7 w	
512 18		514 27	316+196, 264+226
503 5			
497 10		495 17	301+196, 264+226
490 5			
		485 8	
478 17			
		472 18	
463 16		463 15	
448 10	224+224	443 25	
430 27			
414 10		417 22	
405 17		404 8	
392 26		393 15	196+196
377 6		378 33	
368 12		360 30	
356 14		349 11 w	
337 29		333 18	
		317 18	
300 60		300 25	
		283 8 w	
		275 8 w	
266 27		264 12	
		250 25 w	
		230 40 w	
224 16		223 18	
		209 6 w	
191 27			
		196 22	

compare both spectra in more details, we have fitted the low-frequency domain ranging from 200 to 600 cm^{-1} with the same set of lines than that retrieved from the S_1 spectrum. The resulting fit is displayed in Fig. 5(a). The peak frequencies involved in the fit are listed in Table II. In order to fit the lowest modes around 200 cm^{-1}, the curve has been deconvoluted from the Raleigh scattering, which is taken into account by an exponentially decaying curve centered at zero with a width of 45 cm^{-1}. The comparison between the parameters used to fit the S_1-type and S_2-type spectra demonstrates that the same modes are implied in both fits. The slight downshift observed between the frequency values can be interpreted as the result of the additional interaction of the metallofullerenes with the solvent in the S_2-type sample. Very few additional lines contribute to the signal. In order to account for the higher part of the spectrum between 550 and 700 cm^{-1}, one additional C_{60} mode of Hg symmetry has been included, at 775 cm^{-1}. The C_{60}-related mode has a

frequency of 675 cm^{-1}. The large number of modes observed in the 609–780 cm^{-1} region is in agreement with the picture of Hg C_{60}-related mode splitting. One can reasonably suggest that the strong line observed at 609 cm^{-1} corresponds to the predicted Hg(3) C_{60}-related mode.

We now turn to the low-frequency part of the spectrum of $Ti_2@C_{80}$. This spectrum is displayed in Fig. 5(b). The main difference between this spectrum and the corresponding $La_2@C_{80}$ spectrum is the absence of marked structures in the former case. This could be the result of a larger mode splitting, as expected given the fact that the sample is a mixture of the same isomer I_h as in the case of $La_2@C_{80}$ and of the D_{5h} isomer of lower symmetry. The symmetries of the Raman-active modes of D_{5h} group are A_1', E_2', and E_1''. The relevant structure of the dimetallofullerene is C_{2v}. It implies the following splitting of the modes:

$$
\begin{aligned}
A_1' &\rightarrow A_1, \\
A_2' &\rightarrow B_1, \\
E_1' &\rightarrow A_1 + B_1, \\
E_2' &\rightarrow A_1 + B_1, \\
A_1'' &\rightarrow A_2, \\
A_2'' &\rightarrow B_2, \\
E_1'' &\rightarrow A_2 + B_2, \\
E_2'' &\rightarrow A_2 + B_2.
\end{aligned} \tag{3}
$$

The A_1, B_1, and B_2 modes are all Raman active. As in the case of $La_2@C_{80}$, we can expect to relate the observed modes to C_{60} modes, but we also can expect to observe modes that derive from additional C_{70}-related modes since C_{70} has D_{5h} symmetry. Linear fits deduced from these modes are displayed in Fig. 4(b), which also includes the previous C_{60} linear fits. They lead to predict cage modes at 210, 243, 386, 406, 425, 653, and 685 cm^{-1} in addition to the previous C_{60}-related modes. The fit of the spectrum is displayed in Fig. 5(b). Line frequencies and widths are listed in Table II. As previously observed in the high and middle parts of the spectrum, the number of lines necessary to obtain a satisfying fit is not much greater than in the case of the $La_2@C_{80}$ spectrum. Because of the resolution and complexity of the fit, it is nevertheless possible that the broadest lines correspond to unresolved structures. The spectra of both $Ti_2@C_{80}$ and $La_2@C_{80}$ are correctly fitted in the range 180–800 cm^{-1} by about 30 modes. A more detailed analysis of the observed frequencies indicates that, apart from a small shift, all the C_{60}-related modes appear in both the $Ti_2@C_{80}$ and $La_2@C_{80}$ spectra. In the low-frequency part of the former spectrum, two lines at 209 and 250 cm^{-1} have frequencies close to C_{70}-related modes, but the identification of lines with C_{70}-related modes is not obvious for most of them, in contrast to the case of C_{60}-related modes. The influence of the coupling of the cage and ions is more sensitive in the lowest-frequency range of the spectrum. The thin and quite strong line at 196 cm^{-1} observed in the spectrum of $Ti_2@C_{80}$ could be a good candidate for such a fingerprint. The value of the force constant k_1 related to the Ti-cage bond, deduced from Eq. (2) is 1 N/cm. This value is lower but of the same order of magnitude than the values deduced in the case of divalent ions.[15] The titanium atom belongs to the group IV, and its highest ionization state is 4. Nevertheless, the electron energy loss spectroscopy (EELS) spectra of $Ti_2@C_{80}$ reveal that the valence state of Ti in $Ti_2@C_{80}$ is lower or of the order of 2+ (Ref. 12). Our results are in good agreement with this observation. The masses of titanium and lanthanum are in a ratio of nearly 1/3. This large mass difference is partly counterbalanced by a weakest interaction of the titanium ions with the cage. Finally, despite the mass difference of the two different species, the spectra are quite similar in the range 300–700 cm^{-1} in agreement with the fact that the fingerprints of the interaction between the cage and trapped ions are expected in the low-frequency range of the Raman spectrum.

V. CONCLUSION

We have presented a detailed analysis of the Raman features of two dimetallofullerenes. In order to compare these results with those of previous studies of mono- and dimetallofullerenes we have compared the observed frequencies to the predicted values deduced from the empirical mass scale that relates the frequencies of metallofullerenes to C_{60} mode frequencies. We have identified a low-frequency line for each species, which we have tentatively assigned to a metal-cage vibration. The derived values of the ion-cage bond force constants are compatible with a 3+ ionization state of each lanthanum atom inside the C_{80} cage and with an ionization state of 2+ at most for each titanium atom inside the C_{80} cage. They are in agreement with the expected values. This confirms in particular that the ionization state of the group-IV titanium atom is not the highest possible one.

*Corresponding author. Electronic address:
anne.debarre@lac.u-psud.fr

[1] Y. Chai, T. Guo, C. Jin, R. E. Haufler, L. P. F. Chibante, J. Fur, L. Wang, J. M. Alford, and R. E. Smalley, J. Phys. Chem. **95**, 7564 (1991).

[2] S. Stevenson, G. Rice, T. Glass, K. Harich, F. Cromer, M. R. Jordan, J. Craft, E. Hadju, R. Bible, M. M. Olmstead, K. Maitra, A. J. Fischer, A. L. Balch, and H. C. Dorn, Nature (London) **401**, 55 (1999).

[3] H. Shinohara, Rep. Prog. Phys. **63**, 843 (2000).

[4] S. Nagase, K. Kobayashi, T. Akasaka, and T. Wakahara, in *Fullerenes: Chemistry, Physics and Technology*, edited by K. M. Kadich and R. S. Ruoff (Wiley, New York, 2000), Chap. 9, p. 395.

[5] M. Takata, B. Umeda, E. Nishibori, M. Sakata, Y. Saïto, M. Ohno, and H. Shinohara, Nature (London) **377**, 46 (1995).

[6] M. Takata, E. Nishibori, B. Umeda, M. Sakata, E. Yamamoto, and H. Shinohara, Phys. Rev. Lett. **78**, 3330 (1997).

[7] K. Kobayashi and S. Nagase, Chem. Phys. Lett. **302**, 312 (1999).
[8] C. Sarasola, J. M. Elorza, and J. M. Ugalde, Chem. Phys. Lett. **285**, 226 (1998).
[9] K. Sueki, K. Akiyama, K. Kikuchi, and H. Nakahara, Chem. Phys. Lett. **291**, 37 (1998).
[10] S. Lebedkin, B. Renker, R. Heid, H. Schober, and H. Rietschel, Appl. Phys. A: Mater. Sci. Process. **66**, 273 (1998).
[11] M. Krause, M. Hulman, H. Kuzmany, P. Kuran, L. Dunsch, T. J. S. Dennis, M. Inakuma, and H. Shinohara, J. Mol. Struct. **521**, 325 (2000).
[12] Baopeng Cao, Masaki Hasegawa, Kozue Okada, Tetsuo Tomiyama, Toshiya Okazaki, Kazutomo Suenaga, and Hisanori Shinohara, J. Am. Chem. Soc. **123**, 9679 (2001).
[13] K. Iwasaki, T. Miyazaki, S. Hino, D. Yoshimura, B.-P. Cao, T. Okazaki, and H. Shinohara (unpublished).
[14] M. Krause, M. Hulman, H. Kuzmany, T. J. S. Dennis, M. Inakuma, and H. Shinohara, J. Chem. Phys. **111**, 7976 (1999).
[15] M. Inakuma, E. Yamamoto, T. Kai, C.-R. Wang, T. Tomiyama, H. Shinohara, T. J. S. Dennis, M. Hulman, M. Krause, and H. Kuzmany, J. Phys. Chem. B **104**, 5072 (2000).
[16] J. Azoulay, A. Débarre, A. Richard, P. Tchénio, S. Bandow, and S. Iijima, Chem. Phys. Lett. **331**, 347 (2000).
[17] M. M. Alvarez, E. G. Gillian, K. Holczer, R. B. Kaner, K. S. Min, and R. L. Whetten, Chem. Phys. Lett. **196**, 337 (1992).
[18] T. Suzuki, Y. Maruyama, T. Kato, K. Kikuchi, Y. Nakao, Y. Achiba, K. Kobayashi, and S. Nagase, Angew. Chem., Int. Ed. Engl. **34**, 1094 (1995).
[19] K. Kobayashi and S. Nagase, Chem. Phys. Lett. **262**, 227 (1996).
[20] M. S. Dresselhaus, G. Dresselhaus, and R. Saito, Phys. Rev. B **45**, 6234 (1992).
[21] B. W. Smith, D. E. Luzzi, and Y. Achiba, Chem. Phys. Lett. **331**, 137 (2000).
[22] E. Nishibori, M. Takata, M. Sakata, A. Taninaka, and H. Shinohara, Angew. Chem., Int. Ed. Engl. **40**, 2998 (2001).
[23] T. Akasaka, S. Nagasa, K. Kobayashi, M. Wälchli, K. Yamamoto, H. Funasaka, M. Kako, T. Hoshino, and T. Erata, Angew. Chem., Int. Ed. Engl. **36**, 1643 (1997).
[24] P. C. Eklund, A. M. Rao, Y. Wang, P. Zhou, K. A. Wang, J. M. Holden, M. S. Dresselhaus, and G. Dresselhaus, Thin Solid Films **257**, 211 (1995).
[25] V. Schettino, P. R. Salvi, R. Bini, and G. Cardini, J. Chem. Phys. **101**, 11 079 (1994).
[26] F. Negri and G. Orlandi, J. Phys. B **29**, 5049 (1996).
[27] T. A. Beu, J. Onoe, and K. Takeuchi, Eur. Phys. J. D **10**, 391 (2000).
[28] W. Brockner and F. Menzl, J. Mol. Struct. **378**, 147 (1996).
[29] R. A. Jishi, M. S. Dresselhaus, G. Dressehaus, K.-A. Wang, P. Zhou, A. M. Rao, and P. C. Eklund, Chem. Phys. Lett. **206**, 187 (1993).